Proc. Natl. Acad. Sci. USA
Vol. 91, pp. 9549–9553, September 1994
Biophysics

The non-B-DNA structure of d(CA/TG)$_n$ does not differ from that of Z-DNA

(left-handed DNA/statistical mechanics/dinucleotide repeats)

P. SHING HO

Department of Biochemistry and Biophysics, ALS 2011, Oregon State University, Corvallis, OR 97331

Communicated by Alexander Rich, June 17, 1994

ABSTRACT **A number of recent studies have shown that simple repetitive d(CA/TG) dinucleotide sequences adopt a left-handed non-B-DNA structure under negative superhelical stress. The pattern of chemical reactivities and the helical parameters observed for these sequences differ significantly from those of standard Z-DNA. In this study, the data for two naturally occurring d(CA/TG)$_n$ sequences are reevaluated by a statistical mechanics treatment of the B- to Z-DNA transition. The behavior of these sequences under negative superhelical stress is accurately simulated by this model, including the multiple and discrete transitions observed for the rat prolactin promoter. Furthermore, the average helical twist for the left-handed structure of d(CA/TG)$_n$ deviates <2% from that expected for standard Z-DNA. Finally, the predicted distribution of the junctions between B- and Z-DNA are shown to account for differences observed in the patterns of chemical reactivity of d(CA/TG)$_n$ and d(CG)$_n$. Thus, no new left-handed structure that differs from Z-DNA is needed to describe the supercoil-induced conformation in d(CA/TG)$_n$ sequences.**

A large number of simple repetitive DNAs have been found in eukaryotic genomes (1). Sequences that are predominantly d(CA)$_n$d(TG)$_n$ [repeating d(CA/TG) dinucleotides] have been found near a number of eukaryotic genes (2), including human genes (3, 4). The presence of these sequences at the rat prolactin (5) and growth hormone promoter regions (6) along with their absence from prokaryotic genes (7) suggest that this motif is involved in controlling eukaryotic transcription. Studies on the structural transitions of d(CA/TG)$_n$ have thus become increasingly interesting as potential modulators of eukaryotic transcription.

Left-handed Z-DNA has been thought to form in d(CA/TG)$_n$ sequences. Z-DNA is characterized by alternating *anti–syn* conformations of pyrimidine and purine bases, respectively (8). Alternating pyrimidine-purine (APP) sequences such as d(CG)$_n$ and d(CA/TG)$_n$ therefore can potentially adopt the Z conformation. Z-DNA is stabilized by a number of factors including negative supercoiling in closed circular DNA (ccDNA). The structure and thermodynamics for formation of Z-DNA have been studied spectroscopically, by chemical reactivity, antibody binding, and two-dimensional (2-D) gel electrophoresis analyses. The behavior of d(CA/TG)$_n$ differs from that of d(CG)$_n$, the prototypical Z-DNA sequence. However, since it has been clear that d(CA/TG)$_n$ adopts a left-handed conformation, this sequence has generally been assumed to form Z-DNA.

Linear polymers of d(CA/TG)$_n$ adopt a left-handed conformation only under extreme salt conditions (9), even for Z-DNA. Although spectroscopically the left-handed conformations of d(CA/TG)$_n$ and d(CG)$_n$ are different, resonance Raman studies indicate that the structures of the phosphodiester backbones of these polymers are very similar (10). Thus, d(CA/TG)$_n$ is less stable as Z-DNA, but its structure is indistinguishable from that of d(CG)$_n$.

The reactivity of d(CG)$_n$ to conformation-specific reagents is very distinctive. Probes that are specific for unpaired bases react primarily at the junction between B- and Z-DNA (11–13), thus clearly delineating the B–Z junctions. The reactivity patterns of d(CA/TG)$_n$, however, show no clear demarcation of B–Z junctions (14, 15). The standard interpretation is that d(CA/TG)$_n$ requires more supercoiling energy to completely invert to the Z-conformation. Under low superhelical densities, short Z-DNA regions are distributed thermodynamically and/or kinetically throughout the d(CA/TG) sequence (15).

Antibodies, both monoclonal and polyclonal, have been used to probe for Z-DNA in a number of genomes (16–20). These antibodies can be either base specific or conformation specific (17). The lack of sequence specificity of this latter class indicate that the left-handed forms of d(CA/TG)$_n$ and d(CG)$_n$ are not dramatically different, at least in terms of antibody recognition.

The thermodynamic and structural properties of Z-DNA have been best defined from 2-D gel analysis of ccDNA topoisomers containing potential Z-DNA-forming sequences. For d(CG)$_n$, the conversion of B- to Z-DNA (the B–Z transition) is a highly cooperative all-or-none process (21) and gives a structure with a helical repeat that is nearly identical to the −12.0 bp per turn observed in crystal structures (22). Repeating d(CA/TG) dinucleotides under superhelical stress, however, do not show this same degree of helical unwinding, suggesting either that these sequences do not completely invert to Z-DNA or that the left-handed structure of d(CA/TG)$_n$ differs from that of Z-DNA (23). The studies by Johnston *et al.* (15) favor the first interpretation.

Given this body of data, the conclusion drawn by Kladde *et al.* (24), that the left-handed structure of d(CA/TG)$_n$ in supercoiled ccDNA is not that of standard Z-DNA, is both surprising and intriguing. The structure of d(CA/TG)$_n$ in negatively supercoiled ccDNA was described in their studies as being much more open than standard Z-DNA. They observed that d(CA/TG)$_n$ at high negative superhelical densities is more reactive than d(CG)$_n$ to single-strand-specific chemical probes. Furthermore, both the helical unwinding and the cooperativity of the transition observed in naturally occurring d(CA/TG) sequences were significantly less than expected for standard Z-DNA.

Here, the data from chemical reactivity and 2-D gel analyses of d(CA/TG) sequences are reanalyzed by a rigorous statistical mechanics treatment of the zipper model for Z-DNA formation. The behavior of d(CA/TG)$_n$ sequences under negative superhelical stress, including the multiple transitions and the helical twists observed in naturally occurring sequences, are accurately simulated by using only the

The publication costs of this article were defrayed in part by page charge payment. This article must therefore be hereby marked "*advertisement*" in accordance with 18 U.S.C. §1734 solely to indicate this fact.

Abbreviations: APP, alternating pyrimidine-purine; ccDNA, closed circular DNA; 2-D, two-dimensional.

accepted structural and thermodynamic parameters for Z-DNA. Thus, the left-handed conformation of repeating d(CA/TG) sequences is in all respects standard Z-DNA.

METHODS

Zipper Model for the B–Z Transition. The zipper model is a simple description of cooperative transitions between distinct conformations within a biopolymer (21). The model first defines a high-energy nucleation step to initiate the formation of the less stable conformation, followed by a number of lower-energy steps for extending this structure throughout the sequence. For the DNA duplex, this model has been used to analyze the transition from B-DNA to single-stranded DNA (25, 26), cruciforms (27), triple-stranded DNA (28), and Z-DNA (21, 29). For this latter transition, the model describes first the formation of two B–Z junctions, followed by propagation of Z-DNA between the two junctions (Fig. 1).

The structure of the B–Z junction has logically and experimentally been described as a set of unpaired bases. Logically, to abut right-handed B-DNA to left-handed Z-DNA requires a junction having an infinite helical twist (ΔTw). Experimentally, each B–Z junction appears as 4 bp that are sensitive to single-strand-specific nucleases (11) and chemical reagents (12, 30).

The ΔTw and free energies for nucleation (ΔG_N) and propagation (ΔG_P) of Z-DNA can be experimentally determined by 2-D gel electrophoresis studies. In these experiments, a Z-forming sequence is inserted at a specific position of a ccDNA plasmid. A distribution of topoisomers with a broad range of linking numbers relative to relaxed ccDNA (ΔLk) is generated for the plasmid. The formation of Z-DNA is observed as perturbations to the topological properties of the ccDNA.

For each topoisomer, ΔLk partitions between ΔTw and the writhe (ΔWr) according to the relationship ΔLk = ΔTw + ΔWr. Thus, unwinding the DNA by a specific number of helical turns requires that an identical number of negative supercoils be relaxed. Supercoiled ccDNA is a high-energy state. Thus, negative supercoiling can provide the energy to unwind the DNA. Furthermore, the associated relaxing of negative supercoils lowers the overall energy of the ccDNA. This accounts for the stabilization of Z-DNA by negative supercoiling.

In the first dimension of a 2-D gel analysis, topoisomers are resolved according to ΔWr. Topoisomers containing Z-DNA will migrate slower than expected from their ΔLk. The second dimension is run in the presence of an intercalator that relaxes negative supercoils and thus removes the energy that stabilizes Z-DNA. In this dimension, topoisomers migrate according to their intrinsic ΔLk. A B–Z transition is thus observed as a discontinuity in the migration pattern of topoisomers.

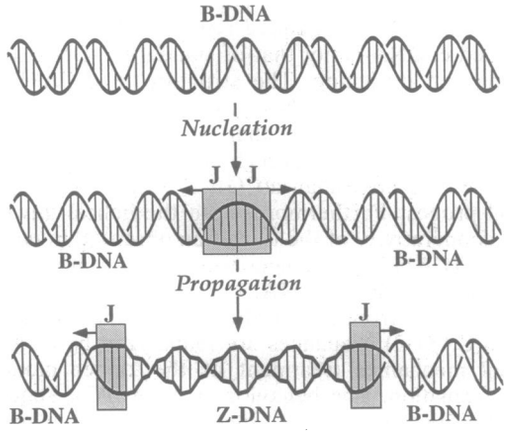

FIG. 1. Two distinct steps of the zipper model for the B–Z transition. The high-energy initial nucleation step involves formation of two B–Z junctions (J), equivalent to 8 unpaired base steps. The propagation of Z-DNA results as the junctions migrate in opposite directions along the chain.

Using this 2-D gel assay, Peck and Wang (21) determined that the nucleation step required a ΔTw = −0.4 turn per junction and a ΔG_N = 5.0 kcal per mol per junction (1 cal = 4.184 J). The propagation of Z-DNA through d(CG) dinucleotides requires a ΔTw = −0.357 turn per dinucleotide (dn) and ΔG_P = 0.6 kcal per mol per dn. By systematically substituting nucleotide bases within $d(CG)_n$ sequences, ΔG_P values have been determined for a number of APP and non-APP dinucleotides (31). For all other dinucleotides, ΔG_P can be estimated from these experimental values (Table 1). Thus, the thermodynamic ability of any sequence to form Z-DNA can be assessed by the zipper model.

Statistical Mechanics Treatment of the B–Z Transition. The transition from B- to Z-DNA can be quantitatively described by applying a statistical mechanics treatment to the zipper model (21, 29). This method assesses the probability of finding Z-DNA at any particular dinucleotide at a given superhelical density (σ) or (ΔLk).

A statistical mechanics treatment starts with a description of the free energies for all possible states of the molecule. The free energy of ccDNA topoisomers is described by the equation $\Delta G^\circ = K\Delta Lk^2$, where $K = 1100RT/N$ for a plasmid N base pairs in size. The extent to which ΔLk partitions between ΔTw and ΔWr depends on ΔG_N and ΔG_P and the number of supercoils relaxed by the structural transition. The partition function (Q) for the B–Z transition (21) for all combinations of dinucleotides is described in Eq. 1 (32). S_j is the equilibrium constant and a_j is the degree of helical unwinding for propagating Z-DNA at the jth dinucleotide. σ is the equilibrium constant and b is the degree of unwinding for the nucleation step

$$Q = 1 + \sum_{i=1}^{n}\sum_{k=1}^{n}\sigma\left(\prod_{j=i}^{k}S_j\right) \times \exp\left\{\frac{-K}{RT}\left[\Delta Lk - \left(\sum_{j=i}^{k}a_j\right) - 2b\right]^2\right\}. \quad [1]$$

The probability of finding Z-DNA in a given sequence can be calculated as ⟨ΔTw⟩ (Eq. 2), which is directly comparable to the ⟨ΔTw⟩ observed in the 2-D gel experiments (32)

$$\langle\Delta Tw\rangle = Q^{-1}\left\{\sum_{i=1}^{n}\sum_{k=1}^{n}\left[\left(\sum_{j=1}^{k}a_j\right) + b\right)\sigma\left(\prod_{j=i}^{k}S_j\right) \times \exp\left[\frac{-K}{RT}\left(\Delta Lk - \left(\sum_{j=i}^{k}a_j\right) - 2b\right)^2\right]\right\}. \quad [2]$$

Table 1. Propagation free energies (ΔG_P, kcal per mol per dn) required to extend Z-DNA after the nucleation step (ΔG_N = 10.0 kcal per mol per dn)

	ΔG_P	Ref.
CG	0.6	21
CA/TG	1.4	29
TA	2.4	32
CC/GG	2.4	33
TC/AG	2.5	33
AA/TT	4.4	31

ΔG_P values are listed for the unique dinucleotides in the optimum *anti–syn* conformations. Values for all combinations including nonideal conformations for Z-DNA are found in ref. 31.

For multiple competing transitions, Q is extended to include the additional conformational states of the DNA (Eq. 3) (33)

$$Q = \left(1 + \sum_{a=1}^{n}\sum_{b=a}^{n} \sigma\left(\prod_{c=a}^{b} S_c\right)\right) \times \left(1 + \sum_{d=1}^{m}\sum_{e=d}^{m} \sigma\left(\prod_{g=d}^{e} S_g\right)\right), \text{ etc.} \quad [3]$$

The program TREZ was used to simulate the behavior of the B–Z transition for multiple competing Z-forming sequences (34). The program Z-HUNT II (4) was used to scan sequences for regions having high propensities to form Z-DNA (Z propensities).

RESULTS

The evidence suggesting that the left-handed conformation of d(CA/TG)$_n$ is not the standard Z-DNA structure typified by d(CG)$_n$ includes (*i*) the reactivity pattern with conformation-sensitive probes is different, (*ii*) the structural transition is not all-or-none, and (*iii*) the helical repeat differs significantly from −12.0 bp per turn. These arguments come primarily from studies on d(CA/TG) repeats found in the rat prolactin promoter (24), which were observed to undergo multiple and discrete transitions to a non-B structure. A helical repeat of −14 to −16 bp per turn was determined for this non-B-DNA structure, which is significantly less left-handed than that of Z-DNA.

For the current study, the established ΔG_N, ΔG_P and helical unwinding parameters for standard Z-DNA are used in a statistical mechanics model to simulate the B–Z transition in d(CA/TG)$_n$ sequences. These results are compared to the transitions observed for the rat somatostatin and prolactin gene promoter regions.

The Non-B-DNA Structure in the Rat Somatostatin and Prolactin Genes. Simple repeats of 25 d(CA/TG) dinucleotides are found at both the 5′ and 3′ ends of the rat somatostatin gene (14). From 2-D gel analysis and S1 nuclease mapping, these sequences were shown to adopt a left-handed structure, presumably that of Z-DNA (14). A comparison to the behavior predicted for a d(CA/TG)$_{25}$ sequence as Z-DNA shows that the statistical mechanics model simulates the 2-D gel results extremely well, both in terms of the ⟨ΔLk⟩ for the transition and the ⟨ΔTw⟩ expected at each topoisomer (Fig. 2*A*). The transition shows an initial unwinding of −6 turns at ⟨ΔLk⟩ = −12 to −15 (≈−2 turns per ΔLk). This is followed by a more gradual unwinding from ⟨ΔLk⟩ = −15 to −20. This simple sequence exhibits a single transition from B- to Z-DNA that is generally cooperative, although not the all-or-none behavior expected for d(CG)$_n$ sequences.

The d(CA/TG)$_{25}$ sequence is observed experimentally and from the statistical mechanics model to never reach the full ⟨ΔTw⟩ (−9.7 turns) expected for Z-DNA at these levels of superhelical densities. Why do d(CA/TG) repeats behave in this manner? According to the zipper model, a true all-or-none transition requires that $\Delta G_P = 0$. The all-or-none B–Z transition in short d(CG)$_n$ sequences results from the low ΔG_P (0.6 kcal per mol per dn) of d(CG) dinucleotides. For d(CA/TG) dinucleotides, ΔG_P is significantly higher (1.4 kcal per mol per dn), and thus the probability for propagating Z-DNA approaches that for nucleation. The B–Z transition for simple d(CA/TG) repeats, therefore, is predicted to be cooperative, but less so than for comparable d(CG) sequences.

The rat prolactin promoter contains 178 bp (at positions −1443 to −1256) and 58 bp (at positions −1925 to −1850) of predominantly alternating d(CA/TG) interrupted by non-APP dinucleotides (24). A statistical mechanics simulation predicts multiple and discrete B–Z transitions for the 178-bp

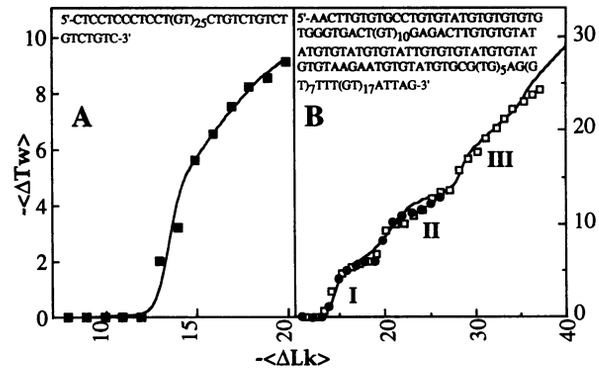

FIG. 2. Change in helical twist (⟨ΔTw⟩) as a function of linking number (⟨ΔLk⟩) for d(CA/TG) repeats. (*A*) Statistical mechanics simulation of the B–Z transition (line) is compared to ⟨ΔTw⟩ extracted from figure 3*C* of Hayes and Dixon (14) (squares) for the d(CA/TG) repeats at the 5′ end of the rat somatostatin sequence in a theoretical 3000-bp plasmid. (*B*) Simulation of the B–Z transition (line) for the 178-bp d(CA/TG) sequence of the rat prolactin gene in a 3272-bp plasmid is compared to the ⟨ΔTw⟩ extracted from the 2-D gels of Kladde *et al.* (24). Solid circles are from figure 2 (run in the presence of 1.75 μg of chloroquine per ml in the second dimension) and open squares are from figure 3 (run with 10 μg of chloroquine per ml) of ref. 24.

sequence (Fig. 2*B*) and matches the ⟨ΔTw⟩ from the two separate 2-D gel experiments reported by Kladde *et al.* (24) remarkably well. The numbers of distinct transitions expected and observed are nearly identical, as are the midpoints of the transitions and the ⟨ΔTw⟩.

The multiple and discrete B–Z transitions in this sequence result again from the higher ΔG_P for d(CA/TG) dinucleotides. A d(CG)$_n$ sequence can be interrupted by a number of non-APP steps without greatly affecting the behavior of the B–Z transition. The high energy for propagating Z-DNA through d(CA/TG) repeats, however, effectively pauses the B–Z transition at intervening non-APP dinucleotides. This leads to multiple and discrete transitions within nonhomogeneous d(CA/TG) sequences.

The calculated ⟨ΔTw⟩ can be used to simulate the actual 2-D gels under the reported experimental conditions (Fig. 3). These simulations faithfully reproduce the general features of the observed migration pattern of topoisomers. In addition, the ⟨ΔTw⟩ at each topoisomer where transitions are observed in the 2-D gels (ΔLk = −13 to −37), deviates from the

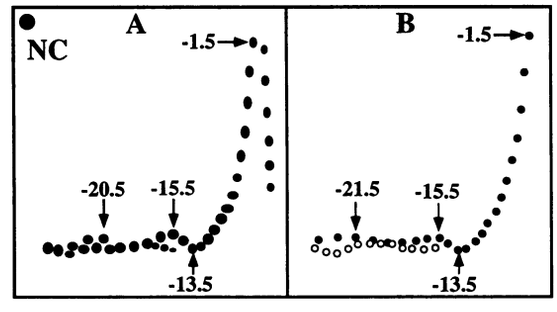

FIG. 3. Simulation of the 2-D gel for the 178-bp d(CA/TG) repeat in the rat prolactin promoter sequence. The topoisomer distribution from figure 3 of Kladde *et al.* (24) (*A*) is compared to the distribution expected (*B*) using the ⟨ΔTw⟩ values calculated for each topoisomer by statistical mechanics (figure 2 of ref. 24). Vertical migration (*Y*; in cm) was simulated by using the empirical function $Y = 14 - \exp[2.81 + 0.17\langle\Delta Wr\rangle]$, where $\langle\Delta Wr\rangle = \langle\Delta Lk\rangle - \langle\Delta Tw\rangle$. Migration of the topoisomers in the horizontal direction (*X*; in cm) was simulated by using the relationship $X = \exp[0.599 - 0.083\langle\Delta Lk\rangle]$ for $\langle\Delta Lk\rangle > -24$ turns (solid circles) and $X = -12.7 - 0.55\ \langle\Delta Lk\rangle$ for $\langle\Delta Lk\rangle < -24$ turns (open circles). NC, nicked closed circular DNA band.

predicted ⟨ΔTw⟩ by an average of −0.2 turn per ΔLk. The average helical repeat of the non-B structure is therefore estimated to be −12.2 bp per turn, which differs from the −12.0 bp per turn of Z-DNA by <2%. Thus, the behavior of the negative supercoiled transition in the rat prolactin promoter can be simulated by using only the accepted thermodynamic and structural parameters for standard Z-DNA.

Using these simulations, we can also define the mechanism for propagating Z-DNA through the rat prolactin promoter sequence. A search through the 178-bp sequence of the rat prolactin promoter (Fig. 4*A*) located three distinct Z-forming regions (Fig. 4*B*). These regions were treated as isolated sequences competing for the unwinding energy in a negatively supercoiled plasmid (Fig. 4*C*). The long stretch of uninterrupted d(CA/TG) dinucleotides at the 3′ end of the promoter was predicted to be the first to undergo a B–Z transition. The transition then proceeds from the 3′ to the 5′ end of the promotor sequence, identical to the progression of the non-B-DNA transition reported by Kladde *et al.* (24). By simply extending Z-DNA from one end of the sequence to the other, only a single pair of high-energy B–Z junctions are required during the entire transition. The propagation to Z-DNA through the sequence is thus an upstream migration of the 5′ junction, pausing at each high-energy non-APP dinucleotide, while holding the junction at the 3′ end fixed.

Reactivity Patterns of d(CA/TG) as Z-DNA. The junctions flanking a Z-DNA-forming sequence are particularly sensitive to enzymes such as S1 nuclease (11) and to chemicals such as hydroxylamine and chloroacetaldehyde (12, 30) that are specific for unpaired bases in DNA. While the B–Z junctions of $d(CG)_n$ are clearly defined by these reagents, the reactivity pattern for $d(CA/TG)_n$ is often complicated. S1 nuclease cleaves the rat somatostatin d(CA/TG) repeats not only at the 5′- and 3′-terminal dinucleotides but extends well into the sequence, including even the central base pairs (14). Kladde *et al.* (24), showed that at $\sigma = -0.05$, chloroacetaldehyde cuts only within a $d(CA)_{31}$ sequence, and not at the flanking regions, as would be expected for Z-DNA. This resulted in the interpretation that the structure of d(CA/TG) is more open than standard Z-DNA.

The statistical model was used to predict the distribution of B–Z junctions across Z-DNA-forming sequences to better understand these reactivity patterns. Fig. 5*A* shows the location of B–Z junctions expected for a $d(CA/TG)_{30}$ sequence at $\sigma = -0.05$ to -0.07. At $\sigma = -0.05$, the B–Z junctions are primarily located within the d(CA/TG) repeats and not at the flanking dinucleotides because <40% (<11/30 dinucleotides on average) of the sequence is expected to be in the Z form. Any junction-specific reagent would thus be expected to react primarily within, and not outside of, the $d(CA/TG)_n$ sequence. This is the pattern of chloroacetaldehyde reactivity reported for a $d(CA/TG)_{31}$ sequence at $\sigma = -0.05$ (24). At higher superhelical densities, the junctions partition toward the flanking dinucleotides. Even at $\sigma = -0.07$, however, there remains a probability of finding junctions within the sequence, as was observed in the hydroxylamine reactivity of $d(CA/TG)_{31}$ (15) and the S1 nuclease digestion of the 5′ $d(CA/TG)_{25}$ sequence of the rat somatostatin gene (14).

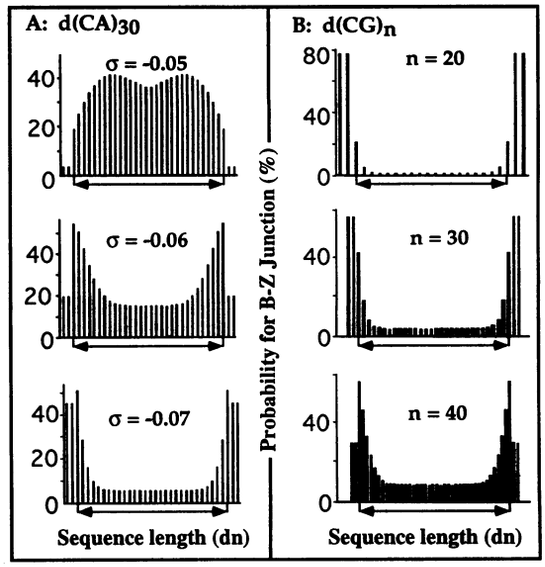

FIG. 5. Predictions for the distribution of B–Z junctions in d(CA/TG) and d(CG) sequences. The probability for locating a B–Z junction was estimated as the product of the probability for not finding Z-DNA at a particular dinucleotide and the Z propensity of the adjacent dinucleotide and the dinucleotide two steps away. The 2 dinucleotides flanking either end of the sequences were assumed to not form Z-DNA but allowed to form junctions. Arrows along the *x* axis indicate the Z-forming d(CA/TG) or d(CG) dinucleotides. (*A*) Probabilities of finding a B–Z junction (%) within a $d(CA/TG)_{30}$ sequence are compared for $\sigma = -0.05$ to -0.07. (*B*) Probabilities of finding a B–Z junction (%) in a $d(CG)_n$ sequence at $\sigma = -0.05$ are compared for $n = 20$–40.

In comparison, the B–Z junctions at $\sigma = -0.05$ are located primarily at the flanking dinucleotides for short $d(CG)_{20}$ and $d(CG)_{30}$ sequences (Fig. 5*B*). Thus, the sequences themselves would be relatively insensitive to single-strand-specific enzymes and chemicals, such as chloroacetaldehyde (24). Only for extremely long sequences ($n >> 30$) will the junctions invade the $d(CG)_n$ regions and partition away from the flanking sequences. These results indicate that reactivity patterns of $d(CA/TG)_n$ and $d(CG)_n$ must be interpreted in the

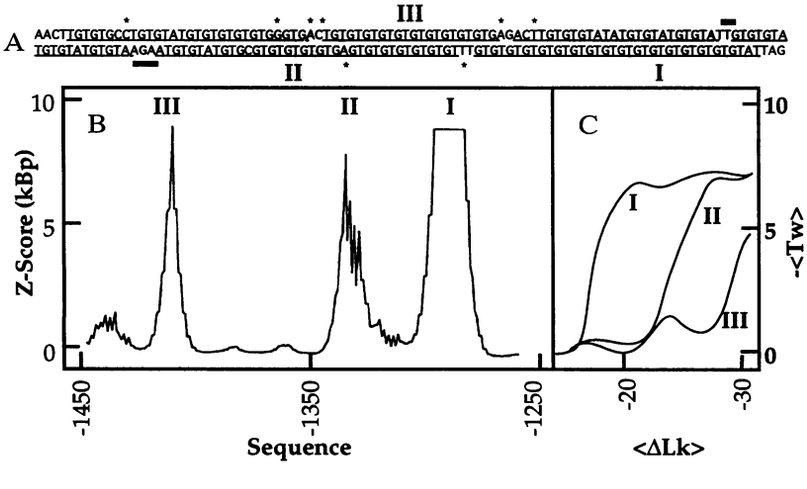

FIG. 4. Predicted behavior of the rat prolactin promoter as Z-DNA. (*A*) Sequence positioned between −1450 and −1250 relative to the transcription start site is shown for the rat prolactin promoter (24). Nearly continuous APP stretches are underlined. Asterisks indicate non-APP steps and solid bars indicate positions where the dinucleotide conformation must be inverted (e.g., from *anti–syn* to *syn–anti*). (*B*) Regions located by Z-HUNT II as having the highest Z-DNA propensities are labeled I, II, and III in this figure and along the sequence. (*C*) Formation of Z-DNA (⟨ΔTw⟩), predicted by TREZ, is plotted relative to the ⟨ΔLk⟩ for a set of topoisomers for a single 3272-bp plasmid containing all three regions (I, II, and III).

context of the sequence, sequence length, and the superhelical density of the ccDNA. The strong correspondence of the predicted distributions of B–Z junctions with the observed reactivity patterns indicate that the structure of d(CA/TG) under superhelical stress does not differ from standard Z-DNA.

DISCUSSION

Simple repeating DNA dinucleotides have been shown to undergo a structural transition to a left-handed conformation under negative superhelical stress. The question addressed by this study is whether $d(CA/TG)_n$ sequences adopt a left-handed conformation that differs from standard Z-DNA. Using a rigorous statistical mechanics treatment of the zipper model for the B–Z transition, it is clear that the change in twist and the degree of cooperativity, including multiple and discrete transitions for nonhomogeneous d(CA/TG) sequences, can be accurately simulated by using only the accepted thermodynamic and structural parameters for Z-DNA. Thus, there is no need for a structural alternative to Z-DNA to describe the left-handed form of naturally occurring $d(CA/TG)_n$ sequences.

One can ask what are the advantages of having complex structural transitions in the promoter region of sequences such as the rat prolactin gene. We had previously considered the potential role of Z-DNA in modulating transcription levels (4) in light of the twin-domain model for transcriptionally induced superhelical stress (35). The model suggests that the mechanics of gene expression induces positive supercoils in front of and negative supercoils behind a transcribing RNA polymerase. This would favor transitions to underwound structures such as Z-DNA upstream of the transcriptional start site. A multiple B–Z transition allows stepwise modulation of DNA topology at the 5′ end of a transcribing gene. The repeating d(CA/TG) sequence of the rat prolactin promoter has been shown to inhibit transcription (36). A stepwise transition to Z-DNA behind the transcribing polymerase could thus regulate the rates of transcription at discrete levels.

This work is dedicated to Dr. Alexander Rich on his 70th birthday. I wish to thank Drs. G. P. Schroth and M. L. Howell and Ms. B. Basham for contributions to the manuscript. This work was supported by grants from the American Cancer Society (NP740B) and the Office of Naval Research (N00014-91-J-1542).

1. Tautz, D. & Renz, M. (1984) *Nucleic Acids Res.* **12,** 4127–4138.
2. Hamada, H., Petrino, M. G. & Kakunaga, T. (1982) *Proc. Natl. Acad. Sci. USA* **79,** 6465–6469.
3. Hamada, H. & Kakunaga, T. (1982) *J. Cell. Biochem.* **3,** Suppl., 333.
4. Schroth, G. P., Chou, P.-J. & Ho, P. S. (1992) *J. Biol. Chem.* **267,** 11846–11855.
5. Maurer, R. A. (1985) *DNA* **4,** 1–9.
6. Thomas, M. J., Freeland, T. M. & Strobl, J. S. (1990) *Mol. Cell. Biol.* **10,** 5378–5387.
7. Gross, D. S. & Garrard, W. T. (1986) *Mol. Cell. Biol.* **6,** 3010–3013.
8. Rich, A., Nordheim, A. & Wang, A. H. J. (1984) in *Annual Review of Physical Chemistry*, ed. Richardson, C. C. (Annual Reviews, Palo Alto, CA), Vol. 16, pp. 791–846.
9. Jovin, T. M., McIntosh, L. P., Arndt Jovin, D. J., Zarling, D. A., Nicoud, M. R., van De Sande, J. H., Jorgenson, K. F. & Eckstein, F. (1983) *J. Biomol. Struct. Dyn.* **1,** 21–58.
10. Klump, H. H., Schmid, E. & Wosgien, M. (1993) *Nucleic Acids Res.* **21,** 2343–2348.
11. Singleton, C. K., Klysik, J., Stirdivant, S. M. & Wells, R. D. (1982) *Nature (London)* **299,** 312–316.
12. Johnston, B. H. & Rich, A. (1985) *Cell* **42,** 713–724.
13. Lilley, D. M. J. & Palecek, E. (1984) *EMBO J.* **3,** 1187–1192.
14. Hayes, T. E. & Dixon, J. E. (1985) *J. Biol. Chem.* **260,** 8145–8156.
15. Johnston, B. H., Ohara, W. & Rich, A. (1988) *J. Biol. Chem.* **263,** 4512–4515.
16. Viegas-Pequignot, E., Derbin, C., Malfoy, B., Taillandier, E., Leng, M. & Dutrillaux, B. (1983) *Proc. Natl. Acad. Sci. USA* **80,** 5890–5894.
17. Nordheim, A., Pardue, M. L., Weiner, L. M., Lowenhaupt, K., Scholten, P., Moeller, A., Rich, A. & Stollar, B. D. (1986) *J. Biol. Chem.* **261,** 468–476.
18. Lancillotti, F., Lopez, M. C., Arias, P. & Alonso, C. (1987) *Proc. Natl. Acad. Sci. USA* **84,** 1560–1564.
19. Wittig, B., Dorbic, T. & Rich, A. (1989) *J. Cell Biol.* **108,** 755–764.
20. Gruskin, E. A. & Rich, A. (1993) *Biochemistry* **32,** 2167–2176.
21. Peck, L. J. & Wang, J. C. (1983) *Proc. Natl. Acad. Sci. USA* **80,** 6206–6210.
22. Wang, A. H. J., Quigley, G. J., Kolpak, F. J., Crawford, J. L., van Boom, J. H., van der Marel, G. & Rich, A. (1979) *Nature (London)* **282,** 680–686.
23. Haniford, D. B. & Pulleyblank, D. E. (1983) *Nature (London)* **302,** 632–634.
24. Kladde, M. P., Kohwi, Y., Kohwi-Shigematsu, T. & Gorksi, J. (1994) *Proc. Natl. Acad. Sci. USA* **91,** 1898–1902.
25. Wetmur, J. G. & Davidson, N. (1968) *J. Mol. Biol.* **31,** 349–370.
26. Record, M. T. & Zimm, B. H. (1972) *Biopolymers* **11,** 1435–1484.
27. Vologodskii, A. V. & Frank-Kamenetskii, M. D. (1982) *FEBS Lett.* **143,** 257–260.
28. Lyamichev, V. I., Mirkin, S. M., Kumarev, V. P., Baranova, L. V., Vologodskii, A. V. & Frank-Kamenetskii, M. D. (1989) *Nucleic Acids Res.* **17,** 9417–9423.
29. Vologodskii, A. V. & Frank-Kamenetskii, M. D. (1984) *J. Biomol. Struct. Dyn.* **1,** 1325–1333.
30. Vogt, N., Marrot, L., Rousseau, N., Malfoy, B. & Leng, M. (1988) *J. Mol. Biol.* **201,** 773–776.
31. Ho, P. S., Ellison, M. J., Quigley, G. J. & Rich, A. (1986) *EMBO J.* **5,** 2737–2744.
32. Ellison, M. J., Feigon, J., Kelleher, R. J., III, Wang, H. J., Habener, J. F. & Rich, A. (1986) *Biochemistry* **25,** 3648–3655.
33. Ellison, M. J., Fenton, M. J., Ho, P. S. & Rich, A. (1987) *EMBO J.* **6,** 1513–1522.
34. Ellison, M. J., Kelleher, R. J., III, Wang, A. H. J., Habener, J. F. & Rich, A. (1985) *Proc. Natl. Acad. Sci. USA* **82,** 8320–8324.
35. Liu, L. F. & Wang, J. C. (1987) *Proc. Natl. Acad. Sci. USA* **84,** 7024–7027.
36. Naylor, L. H. & Clark, E. M. (1990) *Nucleic Acids Res.* **18,** 1595–1601.